*Catalysts* **2015**, *5*, 1603-1621; doi:10.3390/catal5031603

OPEN ACCESS

*catalysts*

**ISSN 2073-4344**

www.mdpi.com/journal/catalysts

*Article*

# Investigation of Room Temperature Synthesis of Titanium Dioxide Nanoclusters Dispersed on Cubic MCM-48 Mesoporous Materials

**Sridhar Budhi [1], Chia-Ming Wu [2], Dan Zhao [3] and Ranjit T. Koodali [2,*]**

[1] Department of Chemistry and Geochemistry, Colorado School of Mines, Golden, CO 80401, USA; E-Mail: budhisridhar@yahoo.co.uk

[2] Department of Chemistry, University of South Dakota, 414 E. Clark Street, Vermillion, SD 57069, USA; E-Mail: chia-ming.wu@coyotes.usd.edu

[3] Department of Chemical Engineering, Ningbo University of Technology, Ningbo 315016, China; E-Mail: zhaodaniccas@nbut.edu.cn

***** Author to whom correspondence should be addressed; E-Mail: ranjit.koodali@usd.edu; Tel.: +1-605-677-6189; Fax: +605-677-6397.

Academic Editor: Keith Hohn

*Received: 2 August 2015 / Accepted: 11 September 2015 / Published: 18 September 2015*

---

**Abstract:** Titania containing cubic MCM-48 mesoporous materials were synthesized successfully at room temperature by a modified Stöber method. The integrity of the cubic mesoporous phase was retained even at relatively high loadings of titania. The $TiO_2$-MCM-48 materials were extensively characterized by a variety of physico-chemical techniques. The physico-chemical characterization indicate that $Ti^{4+}$ ions can be substituted in framework tetrahedral positions. The relative amount of $Ti^{4+}$ ions in tetrahedral position was dependent on the order of addition of the precursor. Even at relatively high loadings of titania, no distinct bulk phase of titania could be observed indicating that the titania nanoclusters are well dispersed on the high surface area mesoporous material and probably exist as amorphous nanoclusters. The $TiO_2$-MCM-48 materials were found to exhibit 100% selectivity in the cyclohexene oxidation at room temperature in the presence of *tert*-butylhydroperoxide (*t*-BHP) as the oxidant. The results suggest that room temperature synthesis is an attractive option for the preparation of $TiO_2$-MCM-48 materials with interesting catalytic properties.

**Keywords:** titanium dioxide; MCM-48; cubic mesoporous materials; cyclohexene; epoxidation

## 1. Introduction

The report of M41S series of periodic mesoporous materials in 1992 spurred excitement and brought a dramatic transformation in the field of porous materials [1,2]. The availability of these types of mesoporous materials, also helped push new frontiers in several interdisciplinary fields, notably catalysis [3], adsorption towards remediation of aqueous pollutants [4], and drug delivery [5]. The discovery has also led to the development of a series of periodic mesoporous materials from prominent groups worldwide, heralding a new era towards the development of porous materials with interesting pore geometries and topologies [6–10].

The M41S series of mesoporous materials comprises of three types, MCM-41, MCM-48, and MCM-50. Among these materials, the cubic MCM-48 material is an interesting material [11,12]. This is because MCM-48 consists of two continuous intersecting network of pores that leads to effective molecular trafficking of reactant(s) and product(s), thus minimizing clogging of pores and leading to enhanced catalytic reactivities in comparison to the uni-dimensional set of pores that occur in $TiO_2$-MCM-41 [13]. Although, MCM-48 is a favorable support material, literature reports regarding its use is lower in comparison to MCM-41. This is because the synthesis of the cubic MCM-48 phase is challenging and is formed only in a narrow range of conditions and is very sensitive to small deviations in the experimental conditions. In addition, the synthesis can be laborious and can take several days [14]. We had reported a facile method for the rapid and reproducible synthesis of MCM-48 [15]. The advantages of this method are that a readily available and common cationic surfactant, cetyltrimethylammonium bromide (CTAB) can be used as the surfactant, thus avoiding the need for the use of specialized gemini surfactants [16], the synthesis can be conducted at room temperature, and the cubic phase can be formed in thirty minutes.

Titanium supported mesoporous materials have attracted the attention of several researchers [17–19]. In particular, the oxidation of aromatics [20,21], oxidation of alkenes [22–28] and unsaturated alcohols [29], and oxidation of thioethers [30] have been successfully demonstrated using titania supported on mesoporous substrates such as MCM-41, SBA-15, MCM-48, *etc*. In contrast to the use of MCM-41 and SBA-15, studies involving MCM-48 as a support to disperse titania nanoclusters for oxidation reactions are relatively scarce.

Titania based MCM-48 materials have been utilized for selective oxidation of styrene [31], 2,6-di-tert-butylphenol [32,33], methyloleate [34], and cyclohexene [25,35–39]. $TiO_2$-MCM-48 prepared by a hydrothermal method was examined for the catalytic oxidation of cyclohexene. The results suggest that the corresponding alcohol, diol, ketone, and epoxide were formed with a selectivity of only 4.7% for cyclohexene oxide [35]. In another study, $TiO_2$-MCM-48 prepared by hydrothermal method and without any sodium ions exhibited higher activity (initial rate being four times higher) for the oxidation of cyclohexene in comparison to a material prepared using sodium ions [36]. However, the paper did not identify the products formed and the selectivity was not reported.

$TiO_2$-MCM-48 was prepared by a hydrothermal method and the oxidation of cyclohexene was carried out under solvent free conditions in the presence of *tert*-butylhydroperoxide (*t*-BHP) as the oxidant. The results indicate that the predominant product was cyclohexene oxide [37]. In another study, $TiO_2$-MCM-48 was prepared by a hydrothermal method at 150 °C for 20 h and using a gemini surfactant. The oxidation of cyclohexene was chosen as a test reaction and the turnover frequency was found to be 5.1 ($h^{-1}$) [38]. The epoxidation of cyclohexene with aqueous hydrogen peroxide over mesostructured $Ti(Cp)_2Cl_2$-grafted $TiO_2$-MCM-48 was examined in another study [39]. It was observed that the $TiO_2$-MCM-48 catalyst exhibited higher activity in comparison to $TiO_2$-MCM-41. Gemini surfactants were used for the preparation of high quality $TiO_2$-MCM-48 mesoporous materials by a hydrothermal method and $TiO_x$ layers were grafted onto the MCM-48 matrix. The turnover number was found to be ~27 after 2 h for the oxidation of cyclohexene [40].

The literature reports pertaining to $TiO_2$-MCM-48 indicate that synthesis methods involve long preparation times and all previous synthetic procedures were conducted under hydrothermal conditions at temperatures >110 °C. It is attractive to pursue synthetic methods for the preparation of $TiO_2$-MCM-48 mesoporous materials at room temperature. However, the synthesis of $TiO_2$-MCM-48 is quite challenging at room temperature. This is because the hydrolysis rates of the titania and silicon alkoxides are significantly different because of differences in the partial charge of the central metal atom, *i.e.*, $Ti^{4+}$ and $Si^{4+}$. The partial charges of $Ti^{4+}$ and $Si^{4+}$ in titanium isopropoxide and tetraethyl orthosilicate are ~+0.61 and +0.32, respectively. This means that titanium isopropoxide undergo hydrolysis at almost twice the rate of tetraethyl orthosilicate. The differences in the rate of the hydrolysis lead to challenges in the reproducible preparation of $TiO_2$-MCM-48. Thus, the preparation of $TiO_2$-MCM-48 is extremely challenging in comparison to the siliceous form of MCM-48 (which in itself is extremely sensitive to the experimental parameters). In this work, we diligently examined the various factors affecting the synthesis, and optimized conditions for the reproducible synthesis of $TiO_2$-MCM-48. In a previous study, we reported the photocatalytic production of hydrogen using $TiO_2$-MCM-48 [41].

Hence, our present work is guided by the following factors: (i) use of a relatively facile method, *i.e.*, room temperature synthesis method for the preparation of $TiO_2$-MCM-48 catalysts thus minimizing synthesis procedures that are quite time-intensive; and (ii) lack of exploration of catalytic oxidation of organics using $TiO_2$-MCM-48 mesoporous catalysts prepared at room temperature. Thus, the present work is expected to provide guidance towards the reproducible room temperature method for the preparation of $TiO_2$-MCM-48 mesoporous materials with different titania loadings and their catalytic performance for oxidation of cyclohexene.

## 2. Results and Discussion

### *2.1. Physico-Chemical Characterization*

As stated earlier, the reproducible and facile synthesis of titania based MCM-48 at room temperature is challenging and hence we examined four different methods for the preparation as discussed in the Experimental Section based on our previous experience [41]. The synthesis method is based on a modified Stöber synthesis developed by us for the preparation of MCM-48 [15]. Figure 1

shows the powder XRD data for the calcined $TiO_2$-MCM-48-200 materials prepared by the four different methods. The diffractograms show XRD patterns typical of the cubic phase with *Ia*3*d* symmetry. The presence of a strong peak near 2θ = 2.5° due to $d_{211}$ diffraction planes and in particular the presence of a weak $d_{220}$ reflection peak near 3.2° is indicative of the presence of the cubic phase. In addition, four additional reflections are seen in the 2θ range of 4° and 6°, suggesting the high quality of the cubic phase. The results suggest that the rapid and facile synthesis method developed by us previous for the synthesis of MCM-48 [15] can be successfully extended to the preparation of $TiO_2$-MCM-48. One can also notice that there are some differences in the Full Width at Half Maxima (FWHM) in the four materials. The FWHM of the diffraction peak is a measure of the size distribution of the unit cell. The two materials, $TiO_2$-MCM-48-B-200 and $TiO_2$-MCM-48-D-200 show relatively smaller FWHM in comparison to the other two materials, $TiO_2$-MCM-48-A-200 and $TiO_2$-MCM-48-C-200. In addition to changes in the FWHM, one can also notice that the preparation methods A and B leads to a relative higher intensity of the $d_{211}$ diffraction plane in comparison to methods, C and D. These differences can be attributed to variations in the order of addition of the precursors, which cause minor changes in the unit cell volume and in the FWHM (*i.e.*, size distribution of the unit cell). Figure 1B shows the long range XRD of all the $TiO_2$-MCM-48-200 materials prepared by the four methods. No peaks due to bulk titania are observed, indicating that the titania nanoclusters are well dispersed and perhaps amorphous and/or crystalline with small crystallite sizes (<3 nm), thus precluding their detection from XRD studies. A broad peak centered at 2θ near 25° can be observed in this material. This peak is assigned to the amorphous silica support.

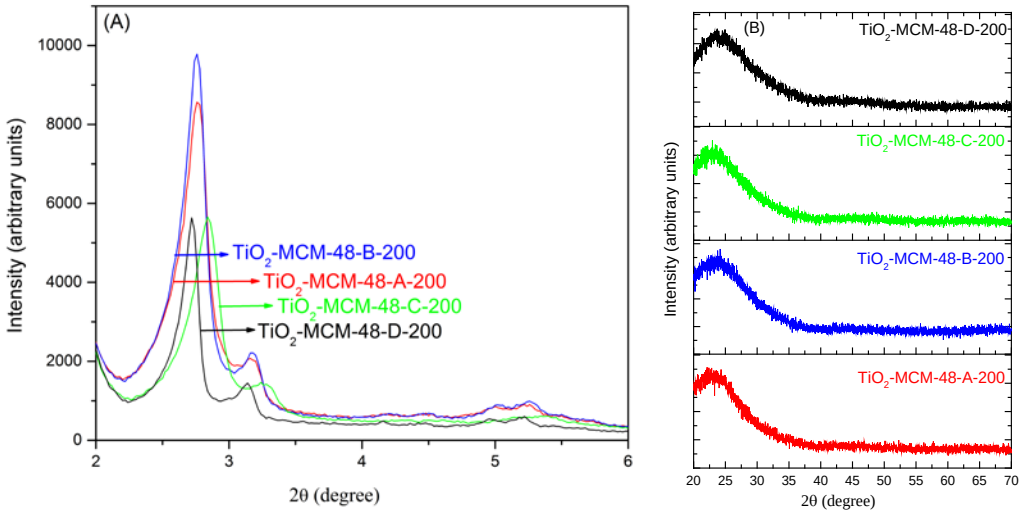


**Figure 1.** XRD patterns of $TiO_2$-MCM-48-200 materials (**A**) short and (**B**) long range.

In summary, the powder XRD studies indicate that high quality cubic phase can be formed at room temperature in as little as four hours. The absence of any peaks due to bulk titania indicate that the titania nanoclusters are amorphous and/or have small crystallite sizes (<3 nm).

We were also interested in preparing $TiO_2$-MCM-48 materials with different titania loadings in order to check if the room temperature synthesis method developed by us can be extended to high loadings of titania. For this purpose, method B (which exhibited the highest specific surface area) was adapted for the preparation of $TiO_2$-MCM-48 materials. The XRD data of $TiO_2$-MCM-48 materials

with different loadings, ranging from Si/Ti = 200 to Si/Ti = 10 is shown in Figure 2. As shown in Figure 2, all materials form the cubic phase, evident from the presence of the small peak near 2θ = 3.2°, that is due to $d_{220}$ diffraction planes. In addition, there are subtle differences in the FWHM and the relative intensity of the peak near 2θ = 2.5°, that is due to $d_{211}$ diffraction planes. These differences can be attributed to the variation in the loading of titania that affects the volume and the size distribution of the unit cell. The inset in Figure 2 shows the long range XRD of $TiO_2$-MCM-48-B-10, *i.e.*, the material with the highest titania loading. The results indicate that even at such high loadings, no peaks due to anatase phase of titania can be seen. This indicates that once again, that the titania nanoclusters are well dispersed on the MCM-48 support. Our results indicate that the intensity of the $d_{211}$ diffraction plane does not monotonically decrease with titania loading suggesting that there are variations in the dispersion of titania in the MCM-48 matrix with increased loadings. The long range XRD of other materials are also similar and are not hence shown. In summary, the powder XRD results indicate that one can prepare $TiO_2$-MCM-48 mesoporous materials with relatively high loadings of titania (e.g., Si/Ti = 10) without destroying the periodicity of the cubic, MCM-48 mesophase even at room temperature. Also, the titania species are well dispersed and perhaps amorphous in nature. Raman studies of these materials also indicate the absence of peaks due to titania indicating the well dispersed and amorphous nature of the titania nanoclusters.

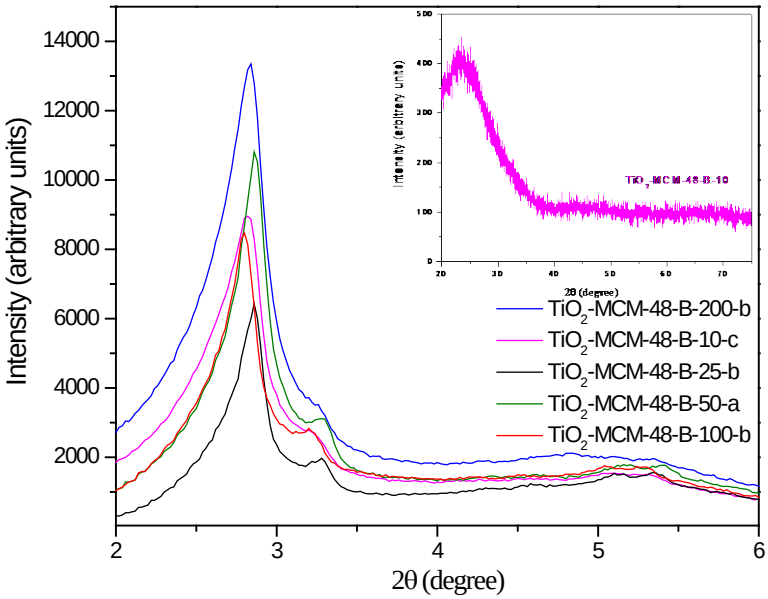


**Figure 2.** The short range powder XRD patterns of $TiO_2$-MCM-48 materials prepared by method B. The inset shows the long range XRD of $TiO_2$-MCM-48-B-10.

Nitrogen adsorption experiments were carried out for all the $TiO_2$-MCM-48 materials at 77 K. Figure 3 presents the nitrogen physisorption isotherms of all $TiO_2$-MCM-48-200 mesoporous materials. The isotherms belong to type IV class of porous materials. This shows the mesoporous nature of pores in these materials. At low relative pressure values ($P/P_0$ < 0.2), monolayer adsorption of nitrogen molecules takes place. At relative pressure ($P/P_0$) values in the range of 0.2 and 0.35, there is a relatively large inflection. This can be attributed to capillary condensation of nitrogen within the mesopores of the MCM-48 material and suggests the presence of highly ordered and periodic

mesoporous nature in these materials. One can also notice that the position of the inflection in all the cubic phased mesoporous materials in this study is similar. This suggests that the pore sizes of these materials are nearly the same as indicated in Table 1. The specific surface area of the materials ranges from 1200 $m^2/g$ to 1687 $m^2/g$ whereas the pore diameter (estimated by using the BJH equation to the desorption isotherm) is nearly 21 Å. The pore volume in this set of materials were found to be >0.7 $cm^3/g$.

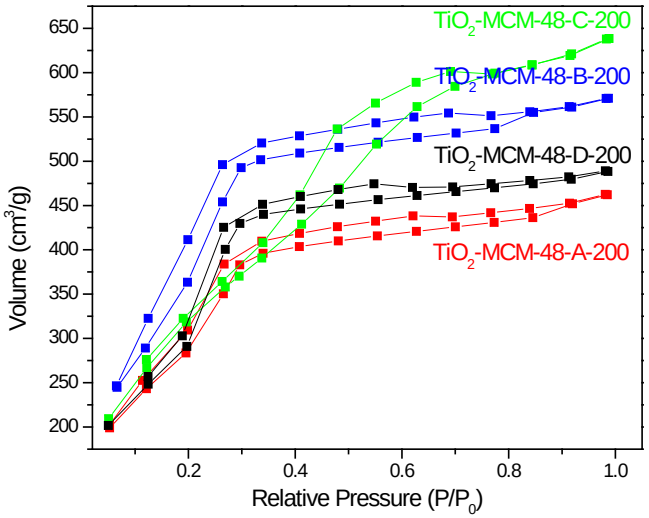


**Figure 3.** Nitrogen isotherms of $TiO_2$-MCM-48-200 materials.

The isotherms of $TiO_2$-MCM-48 mesoporous materials prepared with different titania loadings (Si/Ti = 100, 50, 25, and 10) were similar in nature to the materials with Si/Ti ratio of 200 and are hence not shown. The specific surface area of these materials are in general high, excepting for $TiO_2$-MCM-48-100, that reproducibly and consistently showed lower specific surface area (near 900 $m^2/g$) for reasons unknown at this moment and beyond the scope of this investigation. The pore volumes were in general high (>0.7 $cm^3/g$) excepting for $TiO_2$-MCM-48-100, whereas the pore sizes were fairly uniform and nearly 21 Å irrespective of the loading of titania. A summary of the textural properties is shown in Table 1.

The variations in the physico-chemical properties can be understood as follows. In method A, the titania precursor is added at the very end. In this method, hydrolysis and condensation of silica has already been initiated and a silica-surfactant mesophase has been pre-formed prior to the addition of the titania precursor. Since the composition of the synthesis mixture prior to addition of the titania precursor is an optimized and reported procedure by us previously [15], the addition of an ethanolic solution of the titania precursor at the very end does not significantly affect the quality of the cubic phase. Thus, as indicated previously, a relatively high intensity of the $d_{211}$ plane can be observed for $TiO_2$-MCM-48-A-200 as shown in Figure 1. However, some of the titania nanoclusters can occlude the mesopores because they can precipitate (albeit slowly) under the experimental conditions employed. This results in a relatively lower specific surface area and pore volume. Method D is similar to method A, excepting that titanium alkoxide is used without any dilution. In such a situation, rapid hydrolysis of the titania precursor under the experimental conditions (of high pH) results in occlusion of pores by the titania nanoclusters. This lowers the phase contrast between the pores and the pore

walls and hence the relative intensity of the $d_{211}$ plane is lower as indicated in Figure 1. The pore volumes obtained in methods A and D seem similar with values of ~0.7 $cm^3/g$, while there seems to be differences in the specific surface areas, which are not fully clear at this moment. In method B, titanium alkoxide is added to the cationic surfactant first. This situation is akin to the Evaporation-Induced Self-Assembly (EISA) process. The interactions between the titania oligomers and the CTAB surfactant results in the formation of a hybrid titaniatropic phase of the type, $Ti–OH^+…X^-…CTAB^+$, where $X^-$ represents bromide ions in this work. The silica precursor (negatively charged since the solution pH is ~10.5) interacts with the already formed and well-organized titaniatropic mesophase through the cationic surfactant. Hence, in this method, a highly periodic mesostructure is formed as indicated by powder XRD studies and the specific surface areas are relatively large. In method C, the formation of the titaniatropic mesophase is presumed to be relatively slower in comparison to method B. This is because pre-hydrolysis of titanium alkoxides in polar solvents such as ethanol promotes solvation as explained by us previously [42]. It seems that the titaniatropic mesophase undergoes reorganization through evaporation of the solvent as explained by us in a recent review [43]. This results in a relatively lower quality cubic phase as noted by the fact that the intensity of the $d_{211}$ plane is lower in the material prepared by method C in comparison to method B. In summary, the results suggest that pre-hydrolysis of titanium alkoxide in ethanol (methods B and D) is less preferable since they result in materials with relatively lower textural properties.

Table 1 lists the Si/Ti ratios in the synthesis gel and the actual Si/Ti ratios in the products determined by AAS analyses. The amounts of titania in materials prepared by methods A and C are higher in comparison to methods B and C, indicating that changes in the order of addition also cause variations in the actual amount of titania incorporated onto the cubic MCM-48 matrix. In summary, AAS results indicate that the Si/Ti ratios determined by AAS to be close to the theoretical values, indicating good incorporation of most of the titania precursor on the mesoporous silica support.

**Table 1.** Summary of physico-chemical properties of $TiO_2$-MCM-48 mesoporous materials.

| Catalyst | Si/Ti ratio (Synthesis gel) | Si/Ti ratio (AAS) | Ratio of $Ti_{tet}^{4+}/Ti_{oct}^{4+}$ | Specific Surface Area ($m^2/g$) | Pore Volume ($cm^3/g$) | Pore Diameter (Å) |
|---|---|---|---|---|---|---|
| $TiO_2$-MCM-48-A-200 | 200 | 189 | 1.61 | 1241 | 0.71 | 22 |
| $TiO_2$-MCM-48-B-200 | 200 | 239 | 1.23 | 1687 | 0.98 | 21 |
| $TiO_2$-MCM-48-C-200 | 200 | 177 | 1.51 | 1200 | 0.88 | 23 |
| $TiO_2$-MCM-48-D-200 | 200 | 223 | 1.39 | 1436 | 0.75 | 21 |
| $TiO_2$-MCM-48-B-100 | 100 | 87 | 1.60 | 898 | 0.53 | 20 |
| $TiO_2$-MCM-48-B-50 | 50 | 47 | 1.23 | 1280 | 0.65 | 21 |
| $TiO_2$-MCM-48-B-25 | 25 | 20 | 1.53 | 1563 | 0.82 | 21 |
| $TiO_2$-MCM-48-B-10 | 10 | 13 | 0.91 | 1563 | 0.82 | 24 |

Transmission Electron Microscopic (TEM) studies were conducted for selected mesoporous materials and are shown in Figure 4.

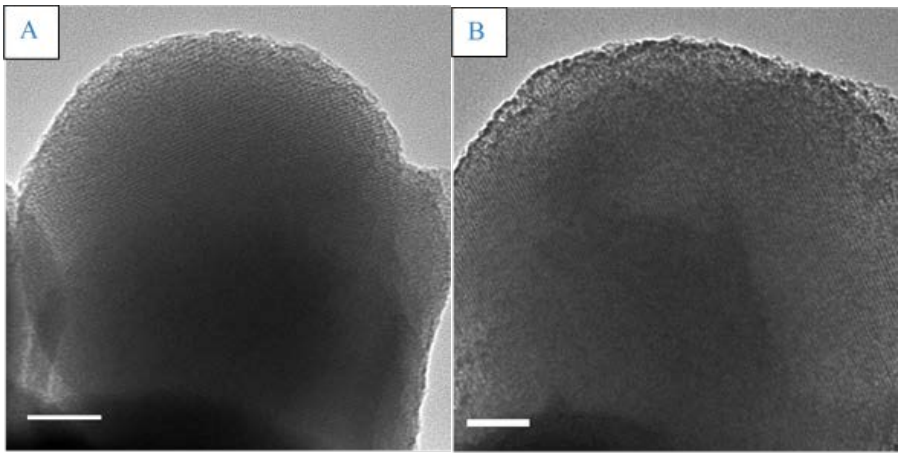


**Figure 4.** Representative TEM images of (**A**) $TiO_2$-MCM-48-B-200 (**left**) and (**B**) $TiO_2$-MCM-48-B-10 (**right**). The bar scale is 50 nm.

Figure 4 shows representative TEM images of $TiO_2$-MCM-48-B-200 and $TiO_2$-MCM-48-B-10 with Si/Ti ratios of 200 and 10. The materials exhibit long-range ordered cubic-typed pore structure of MCM-48. The incorporation of titania did not influence the morphology and the integrity of the pore structure even at high loadings, and is thus consistent with the results obtained from powder XRD studies. A low magnification image of a representative cubic MCM-48 material is shown in Figure S1 indicating the nearly spherical shapes of the mesoporous materials. The bicontinuous and interpenetrating network of pores in MCM-48 poses unique and inherent challenges in imaging the cubic materials from our experiences. A relatively high magnification of a representative titania containing material is shown in Figure S2. The TEM images do not indicate the presence of any crystalline phase of titania in the $TiO_2$-MCM-48-B-10 material suggesting that the titania nanoclusters are perhaps amorphous. In addition, our TEM images do not indicate the presence of any large and aggregated titania particles in the $TiO_2$-MCM-48-200 set of materials. Our results are consistent with previous reports by Gies *et al.* [44]. In their work, despite relatively high loadings of titania, (13–16 wt. %), no large titania particles could be observed from their TEM studies. Our TEM data is consistent with UV-Vis Diffuse Reflectance Spectra (DRS) results that are discussed later. The absence of peaks near 370 nm due to bulk titania is a further confirmation of the absence of large titania crystals [44]. In summary, TEM studies indicate that the titania species are well dispersed on the cubic mesoporous support and probably are amorphous in nature.

Electron Spin Resonance (ESR) studies were conducted in order to better understand the geometry of the titania species. The $TiO_2$-MCM-48 mesoporous materials were illuminated in the presence of methanol as the sacrificial hole scavenger to suppress charge-carrier recombination. Figure 5 shows the ESR spectra of Ti-MCM-8 materials prepared by method B after UV irradiation at 77 K for 10 min. The ESR spectra were measured in the dark at 4.5 K. The samples were ESR silent prior to irradiation. A strong signal near $g$ = 2.004 is observed in all spectra and is this is due to organic radicals (predominantly $\bullet CH_2OH$ with a ratio of 1:2:1) formed by the reaction of the photogenerated holes in $TiO_2$-MCM-48 materials with methanol. The ESR spectra of $TiO_2$-MCM-48 mesoporous materials with Si/Ti ratio of 200 indicate the presence of $Ti^{3+}$ species (Figure 5) with $g_{\perp}$ = 1.951 and $g_{\parallel}$ = 1.910. We have previously observed two sets of ESR signals (signal A and B) in $TiO_2$-MCM-48

materials prepared by first impregnating MCM-48 with titanium isopropoxide and then calcining at 550 °C [13]. Signal A with $g_{\perp}$ = 1.952 and $g_{\parallel}$ = 1.902 was attributed to titanium atoms in tetrahedral coordination in accordance with prior literature [45]. In addition, signal B, with $g_{\perp}$ = 1.988 and $g_{\parallel}$ = 1.957 was attributed to titanium atoms in distorted octahedral coordination. The presence of broad (albeit weak) signals in this study with *g* values similar to previous reports indicates the presence of titanium ions predominantly in tetrahedral coordination at low titania loadings (Si/Ti = 200) [46–48]. The presence of fairly broad and weak peaks precludes us from clearly observing the presence of titanium ions in octahedral coordination. Thus, we performed Diffuse Reflectance Spectroscopic (DRS) studies.

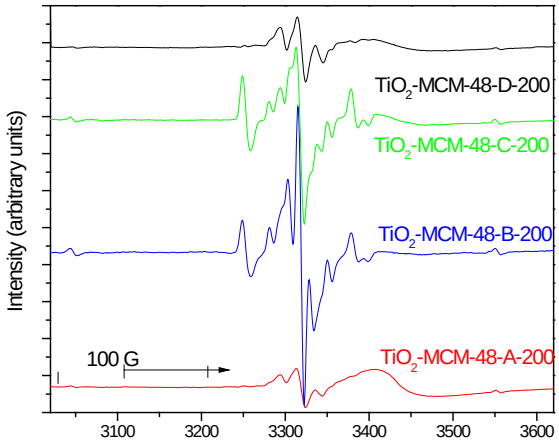


**Figure 5.** ESR spectra of $TiO_2$-MCM-48-200 materials prepared by four different methods.

The UV-Vis DRS spectra of the $TiO_2$-MCM-48-200 materials are shown in Figure 6A–D. Peaks in the 210 to 230 nm range have been previously attributed to ligand-to-metal charge-transfer (LMCT) from $O^{2-}$ to $Ti^{4+}$ due to the presence of tetrahedrally coordinated $Ti^{4+}$ ions [13,41], whereas the presence of octahedrally coordinated $Ti^{4+}$ ions (or highly dispersed titania nanoparticles) can be discerned from the appearance of a peak in the 280 to 310 nm range. In order to identify the relative ratios of the $Ti^{4+}$ ions in tetrahedral and octahedral coordination, the DRS bands were de-convoluted using Origin Pro 9.0 software (OriginLab Corporation, Northampton, MA, USA). The peak centers were fixed at 220 and 280 nm, respectively, for $Ti^{4+}$ ions in tetrahedral and octahedral geometry. The relative ratios of $Ti^{4+}$ ions in tetrahedral and octahedral coordination was then estimated by calculating the peak intensity from the baseline to the top of the peak center with width fixed at 220 ± 10 nm and 280 ± 10 nm in $TiO_2$-MCM-48-A-200, $TiO_2$-MCM-48-C-200, and $TiO_2$-MCM-48-D-200 as reported by us previously [49]. In $TiO_2$-MCM-48-B-200, the peak center with width was fixed at 220 ± 10 nm and 300 ± 10 nm. This suggests that slightly larger sized titania nanoparticles are formed in this material in comparison to the remaining three materials. Table 1 provides a summary of the ratio of $Ti_{tet}^{4+}/Ti_{oct}^{4+}$ for $TiO_2$-MCM-48-200 mesoporous materials. The ratio of $Ti_{tet}^{4+}/Ti_{oct}^{4+}$ in $TiO_2$-MCM-48-A-200, $TiO_2$-MCM-48-B-200, $TiO_2$-MCM-48-C-200, and $TiO_2$-MCM-48-D-200 was estimated to be 1.61, 1.23, 1.51, and 1.39, respectively, suggesting that the method of preparation modulates the amount of $Ti^{4+}$ ions that can be incorporated into the framework tetrahedral positions in the cubic MCM-48 material.

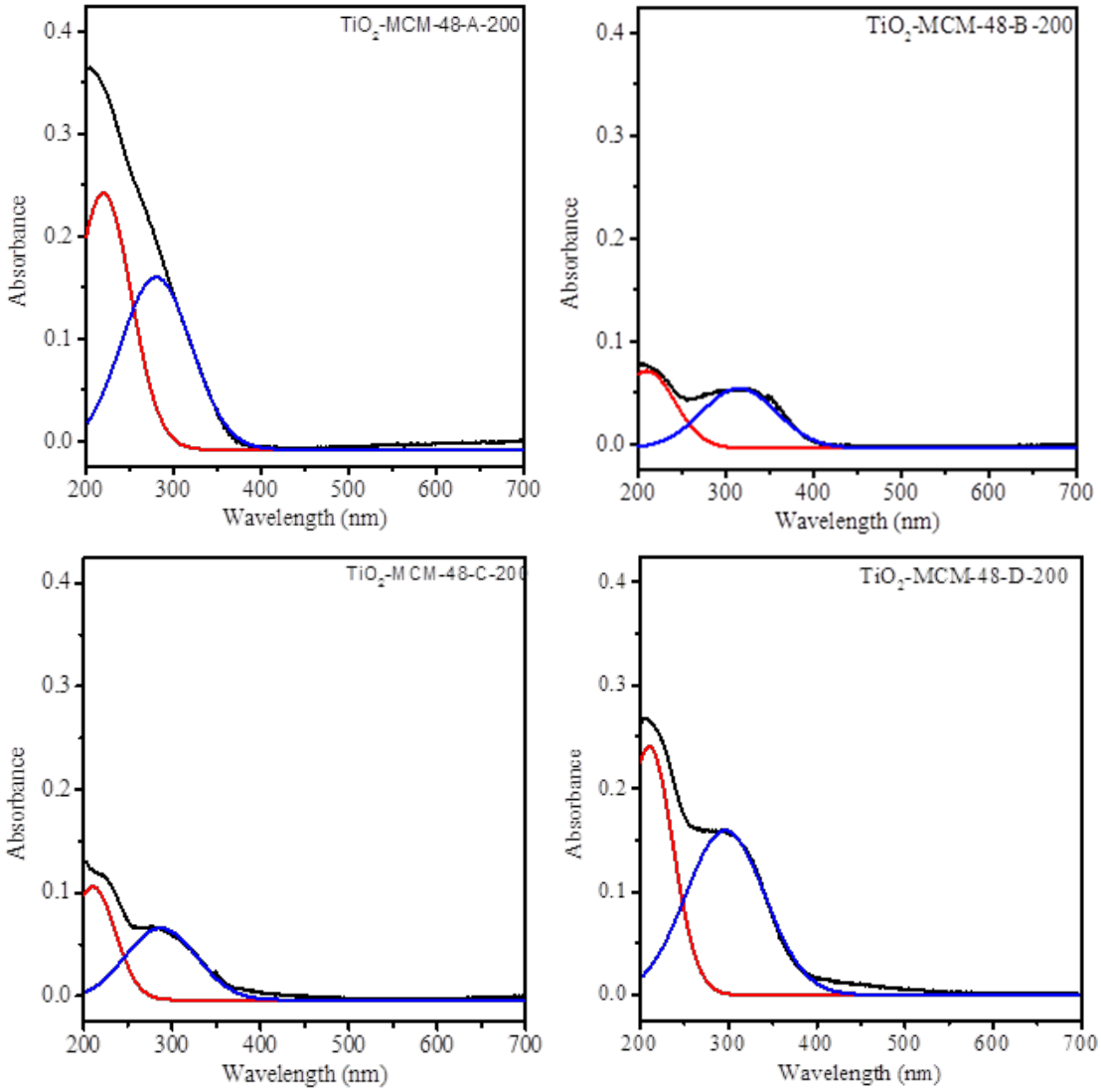


**Figure 6.** UV-Vis DRS of $TiO_2$-MCM-48-200 materials prepared by four different methods. The bold black line shows the original UV-Vis spectra whereas the red and blue bold lines indicate the de-convoluted spectra.

The UV-Vis DR spectra of $TiO_2$-MCM-48 with different loadings are shown in Figure 7 below. In general, one notices that there is a slight red shift in the onset of absorbance with increase in titania loading and also the obvious fact that there is also an increase in the absorbance values with increase in titania. De-convolution of the peaks indicate that the ratio of $Ti_{tet}^{4+}/Ti_{oct}^{4+}$ in $TiO_2$-MCM-48-10 is significantly lower in comparison to the rest of the four samples suggesting that formation of small sized titania clusters at such high loadings (*i.e.*, Si/Ti = 10). The titania clusters are fairly small in size and are probably amorphous too and are thus not seen in powder XRD studies.

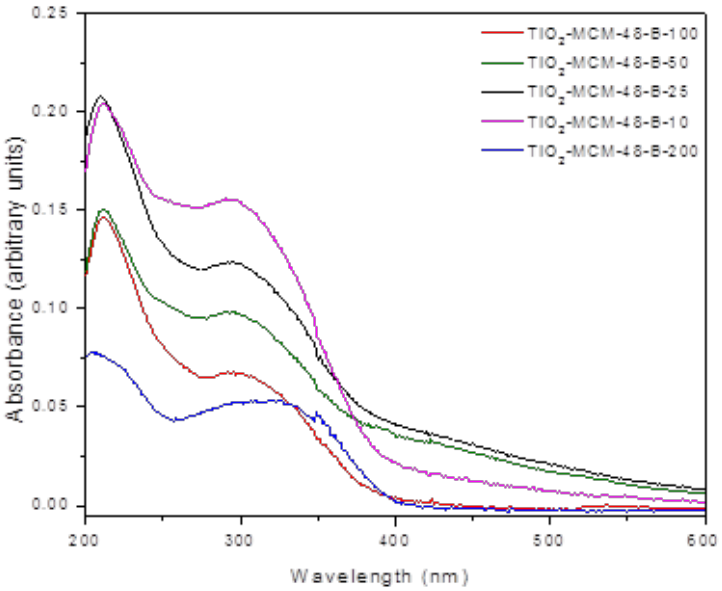


**Figure 7.** UV-Vis DR spectra of $TiO_2$-MCM-48-materials with different titania loadings.

*2.2. Catalytic Studies*

Oxidation reactions have been carried out using microporous TS-1 catalysts [22,46,47]. In contrast to crystalline TS-1 catalysts, the atomic ordering of the pore walls in mesoporous MCM-41 and MCM-48 type materials are amorphous. This often results in conversions and selectivities quite different in the mesoporous materials. $TiO_2$ containing mesoporous materials show catalytic activity for selective oxidation of organics using hydrogen peroxide or *tert*-butylhydroperoxide (*t*-BHP) under relatively mild conditions. In the present study, we examined the oxidation of cyclohexene using the $TiO_2$-MCM-48 materials prepared in this study. Preliminary catalytic experiments indicated that a molar ratio of cyclohexene: *t*-BHP = 1:1 was ideal. In addition, the optimal reaction temperature was found to be 25 ± 5 °C, and dichloroethane was the best solvent under the experimental conditions in this study. Control experiments with siliceous MCM-48 and a Degussa P25 indicate no conversion of cyclohexene even after 24 h of reaction indicating that well dispersed titania is essential for oxidation of cyclohexene.

Our initial catalytic experiments were carried out with the materials with low titania loadings since it has been reported that spatially isolated and tetrahedrally coordinated $Ti^{4+}$ show relatively high activity [50]. We found that the catalytic activity for the oxidation of cyclohexene to be in the order, $TiO_2$-MCM-48-B-200 > $TiO_2$-MCM-48-A-200 > $TiO_2$-MCM-48-C-200 > $TiO_2$-MCM-48-D-200 as indicated in Figure 8.

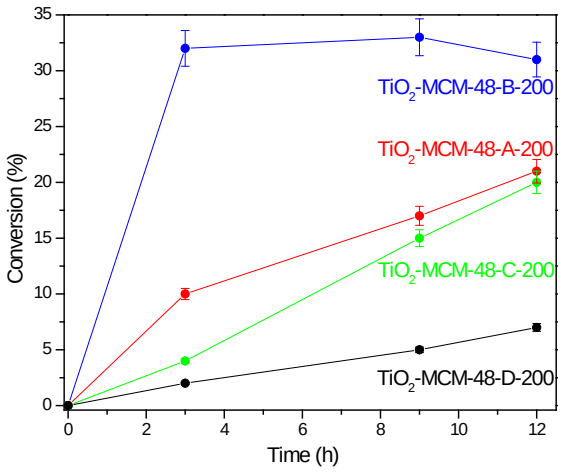


**Figure 8.** Conversion of cyclohexene over various $TiO_2$-MCM-48-200 catalysts.

Interestingly, all catalysts showed exclusive and 100% selectivity for the formation of cyclohexene oxide, contrary to a previous report in which other products have been identified [38]. The turnover number (moles of cyclohexene converted/mol Ti) after 12 h of reaction at room temperature was estimated to be 59, 32, 28, and 21 for $TiO_2$-MCM-48-B-200, $TiO_2$-MCM-48-A-200, $TiO_2$-MCM-48-C-200, and $TiO_2$-MCM-48-D-200 catalysts, respectively. The activity of $TiO_2$-MCM-48-B-200 (turnover number = 59 after 12 h) seems to be better than the activity of microporous TS-1 (turnover number = 47 after 24 h) previously reported under similar conditions [38], suggesting that the room temperature synthesis of $TiO_2$-MCM-48 materials is attractive for catalytic oxidation reactions. The ratio of $Ti_{tet}^{4+}/Ti_{oct}^{4+}$ was calculated to be 1.61, 1.23, 1.51, and 1.39 for $TiO_2$-MCM-48-B-200, $TiO_2$-MCM-48-A-200, $TiO_2$-MCM-48-C-200, and $TiO_2$-MCM-48-D-200, respectively, suggesting that the relative amount of $Ti_{tet}^{4+}$ alone does not dictate the trends in catalytic activity. Indeed, Tuel and Hubert-Pfalzgraf have suggested that the coordination of the titania species may not be the only factor, and that other parameters such as dispersion and particle size of the titania nanoparticle may also play a vital role [51]. This is supported by the fact that Hutter *et al*. found that well dispersed titania nanodomains on $TiO_2$-$SiO_2$ are active for the epoxidation of cyclohexene [52]. Thus, our results are consistent with previous reports and that the presence of nanoclusters of titania do not necessarily decrease the catalytic performance (at least at low loadings of titania). Figure S3 shows a plot of specific surface area and ratio of $Ti_{tet}^{4+}/Ti_{oct}^{4+}$ as a function of turnover number. It seems that the high activity of $TiO_2$-MCM-48-B-200 is due to the relatively high specific surface area and pore volume of this material in comparison to the rest of the materials and hence the high dispersion of titania seems to be responsible for enhancing its activity. No strong correlation seems with the relative amount of $Ti_{tet}^{4+}$ as stated previously.

The recycling studies with $TiO_2$-MCM-48-B-200 indicate a modest decrease in activity after two cycles. Powder XRD analysis of the spent catalyst indicates that the cubic phase is still preserved and the textural properties do not seem to be compromised. We also found that the turnover number of the catalyst decreased progressively with increase in the amount of $TiO_2$ loading. The turnover number was calculated to be 13, 3, 3, and 2.5 for $TiO_2$-MCM-48-B-100, $TiO_2$-MCM-48-B-50, $TiO_2$-MCM-48-B-25, and $TiO_2$-MCM-48-B-10, respectively, suggesting that the decrease in dispersion of titania was perhaps responsible for the decrease in catalytic activity. Interestingly,

contrary to a previous report [53], we did not see any change in the selectivity towards the formation of cyclohexene oxide at high loadings of titania.

In summary, our catalytic results indicate that high selectivity and good activity can be obtained with titania nanoparticles dispersed on a cubic MCM-48 mesoporous support for the epoxidation of cyclohexene even at room temperature.

## 3. Experimental Section

### *3.1. Chemicals Used*

The materials used for the synthesis of $TiO_2$-MCM-48 are ethanol (absolute 200 Proof, AAPER), tetraethyl orthosilicate ($Si(OEt)_4$, 98%, Alfa Aesar, Ward Hill, MA, USA), titanium(IV) isopropoxide (Ti-($^i$OPr)$_4$, 98%, Alfa Aesar), cetyltrimethylammonium bromide (CTAB, 98%, Alfa Aaser), aq. Ammonia (Alfa Aesar). Deionized water was used throughout the studies. For the catalytic studies cyclohexene (99%, Acros, New Jersey, NJ, USA), dichloroethane (Acros), *tert*-butylhydroperoxide, and nonane (99%, Acros) as an internal standard were used.

### *3.2. Synthesis of $TiO_2$-MCM-48 Mesoporous Materials*

A scheme for the four different methods for the preparation of $TiO_2$-MCM-48 is shown in Table 2 below.

**Table 2.** Preparation of $TiO_2$-MCM-48 by different methods.

| Method A | Method B | Method C | Method D |
|---|---|---|---|
| CTAB (1.2 g) | CTAB (1.2 g) | CTAB (1.2 g) | CTAB (1.2 g) |
| $H_2O$ (50 mL) | Ti-($^i$OPr)$_4$ | Ti-($^i$OPr)$_4$ (Stock) * | $H_2O$ (50 mL) |
| $C_2H_5OH$ (25 mL) | $H_2O$ (50 mL) | $H_2O$ (50 mL) | $C_2H_5OH$ (25 mL) |
| $NH_3$ (6 mL) | $C_2H_5OH$ (25 mL) | $C_2H_5OH$ (25 mL) | $NH_3$ (6 mL) |
| $Si(OEt)_4$ (1.8 mL) | $NH_3$ (6 mL) | $NH_3$ (6 mL) | $Si(OEt)_4$ (1.8 mL) |
| Ti-($^i$OPr)$_4$ (Stock)* | $Si(OEt)_4$ (1.8 mL) | $Si(OEt)_4$ (1.8 mL) | Ti-($^i$OPr)$_4$ |

* Preparation of stock solution: For Si/Ti = 200, 70 µL of Ti ($^i$OPr)$_4$ was dissolved in 10 mL of ethanol. This served as the stock solution. One milliliter of this stock solution was used for preparing $TiO_2$-MCM-48 with a Si/Ti ratio of 200.

In a 120 polypropylene beaker, 1.2 g (3.3 mmol) of CTAB were added to 50 mL of deionized water and CTAB was allowed to dissolve fully by stirring rapidly for a few min. Then, 25 mL of ethanol were added to the CTAB solution. To this mixture, 6 mL (0.09 mmol) of aqueous ammonia and the silica precursor, TEOS 1.8 mL were added. The titanium precursor (Ti-($^i$OPr)$_4$ was dissolved in 10 mL of ethanol and served as the stock solution. In method A, 1 mL of the stock solution of Ti-($^i$OPr)$_4$ was added at the very end as shown in Table 2. In method B, the required amount of Ti-($^i$OPr)$_4$ solution (without dilution) was added to the CTAB solution as indicated in the Scheme below. In method C, the stock solution of Ti-($^i$OPr)$_4$ was added after the addition of CTAB. In method D, Ti-($^i$OPr)$_4$ (without dilution) was added to $Si(OEt)_4$ solution. After the addition of all the ingredients, the mixture was stirred for 4 h at 300 rpm at room temperature and the resulting $TiO_2$-MCM-48 was recovered by

filtration, dried in an oven overnight, and then calcined at a heating rate of 3 °C/min at 550 °C for 6 h to remove the organic template. The mesoporous material, $TiO_2$-MCM-48 prepared with a Si/Ti ratio of 200 by method A is named as $TiO_2$-MCM-48-A-200. Other materials prepared in this work are named in a similar manner.

### *3.3. Characterization Techniques*

Powder X-ray diffraction (XRD) measurements were done using a Rigaku Ultima IV X-ray diffractometer (Rigaku Corporation, Tokyo, Japan) with Cu Kα radiation (λ = 1.5408 Å) at room temperature. The diffractometer was typically operated at 1.76 kW (Voltage = 44 kV and Current = 40 mA) and scanned with a step size of 0.02°. The low angle regions were scanned from 2θ = 2°–6° with a step size of 0.02°. Wide angle XRD measurements were also made for selected mesoporous materials in the 2θ range of 20°–75°.

The nitrogen physisorption studies were done at 77 K using Nova 2200*e* analyzer (Quantachrome Instruments, Boynton Beach, FL, USA). The materials were dried in an oven at 373 K for overnight prior to the day of analysis. The materials were then degassed at 373 K extensively before the study. The Brunauer-Emmett-Teller (BET) equation was used to calculate the specific surface area from the adsorption data obtained at relative pressure $P/P_0$ values between 0.05–0.30. The total pore volume of $TiO_2$-MCM-48 mesoporous materials were calculated from the amount of nitrogen adsorbed at highest relative pressure ratio $P/P_0 \sim 0.99$. The pore size distribution was calculated by analyzing the $N_2$ isotherm using the Barrett-Joyner-Halenda (BJH) method and by applying the BJH equation to the desorption isotherm.

Transmission electron microscopic (TEM) images were acquired using a FEI Tecnai $G^2$ F30 instrument (FEI, Hillsboro, TX, USA) at an accelerating voltage of 200 kV. The materials for TEM studies were prepared by first sonicating ~2 mg of $TiO_2$-MCM-48 in 10 mL of ethanol for at least 30 min. One drop of this dispersion was carefully deposited on a carbon coated copper grid (200 mesh). The grid was allowed to dry at room temperature overnight before TEM analysis.

The Electron Spin Resonance (ESR) experiments were conducted in the X-band (continuous wave) using a Bruker Elexsys E580 spectrometer (Bruker, Billerica, MA, USA). This instrument was equipped with an Oxford CF935 helium flow cryostat and a ITC-5025 temperature controller (Oxford Instruments, Oxfordshire, UK). The mesoporous materials were dispersed in water-methanol mixture and were purged with argon gas to remove oxygen. The suspension was then illuminated at 77 K using a 300-W Xe UV lamp source (ILC) (Newport Corporation, Santa Clara, CA, USA). The EPR spectra were then recorded immediately at 5 K immediately after illumination. The $g$ factors were calibrated by comparison to a coal standard, with $g = 2.00285 \pm 0.00005$.

The UV-Vis diffuse reflectance spectra were recorded using a Cary 100 Bio UV-Visible spectrophotometer (Varian Inc., Palo Alto, CA, USA). This instrument was equipped with a praying mantis diffuse reflection accessory (Harrick Scientific). A Si-MCM-48 material was used for baseline correction and the DR spectra were recorded at room temperature.

A Thermo Jarrell Ash Atomic Absorption (Thermo Jarrell Ash Corporation, Franklin, MA, USA) Spectrophotometer was used to determine the titanium content present in the calcined $TiO_2$-MCM-48 materials prepared by different methods and different Si/Ti ratios after dissolution of the materials in

HF:$HNO_3$ solution. The silica was carefully filtered, and the supernatant solution was diluted to known volumes. The solutions were analyzed for $Ti^{4+}$ ions.

The catalytic reactions were performed as described in the following manner. In a typical catalytic reaction, 19.3 mL of dichloroethane (DCE) was added to a single-neck round bottom flask. To this, *tert*-butylhydroperoxide (*t*-BHP, 0.32 mL, 2 mmol) in decane was added and reaction mixture was stirred for 15 min. Then, 0.06 g of the $TiO_2$-MCM-48 catalyst, nonane (0.2 mL), and cyclohexene (0.2 mL, 2 mmol) were added, respectively. The suspension was refluxed at room temperature (25 ± 5 °C) for various intervals of time. After the completion of the reaction, the catalyst was recovered, washed with acetone, and dried in an air oven at 80 ± 10 °C. The supernatant solution (after separation of the catalyst) was injected into a GC-MS (Shimadzu QP 5000, Shimadzu Corporation, Kyoto, Japan). The GC was equipped with a silica column (J&W Scientific, Folsom, CA, USA, 122-5532, DB-5ms equivalent to a (5% phenyl)methyl polysiloxane, 30 m × 0.25 mm). The yield of the product (cyclohexene oxide) was determined using the internal standard method. After the catalytic reaction, the suspension was centrifuged and the catalyst was recovered. This was then washed with acetone and then subsequently dried in air, and tested for recycling experiments.

## 4. Conclusions

Room temperature synthesis of titania supported cubic MCM-48 mesoporous materials were successfully demonstrated. It was found that the order of addition of the titania precursor modulated the relative amount of $Ti^{4+}$ ions in tetrahedral and octahedral coordination. The results indicate that the titania nanoclusters are well dispersed in the high surface area mesoporous matrix and no bulk phase of titania was detected even at relatively high titania loadings. The titania supported MCM-48 materials show excellent selectivity towards the formation of cyclohexene oxide from cyclohexene at room temperature using *tert*-butylhydroperoxide as the oxidant.

## Acknowledgments

Ranjit T. Koodali thanks the South Dakota Center for Research and Development of Light-Activated Materials (CRDLM). We are thankful to Nada Dimitrijevic and Tijana Rajh, Argonne National Laboratory for help with ESR studies. Support from NSF-EPSCoR (EPS-0554609), NSF-CHE-0840507, and NSF-CHE-0722632 are gratefully acknowledged.

## Author Contributions

All authors in this study were involved in the design of the experiments. Sridhar Budhi was primarily involved in the synthesis and catalytic studies; Dan Zhao and Chia-Ming Wu were involved in the characterization and analysis of data. All authors read and approved the final version of the manuscript.

## Conflicts of Interest

The authors declare no conflict of interest.

## References


1. Beck, J.S.; Vartuli, J.C.; Roth, W.J.; Leonowicz, M.E.; Kresge, C.T.; Schmitt, K.D.; Chu, C.T.W.; Olson, D.H.; Sheppard, E.W.; McCullen, S.B.; *et al.* A new family of mesoporous molecular-sieves prepared with liquid-crystal templates. *J. Am. Chem. Soc.* **1992**, *114*, 10834–10843.
2. Kresge, C.T.; Leonowicz, M.E.; Roth, W.J.; Vartuli, J.C.; Beck, J.S. Ordered mesoporous molecular-sieves synthesized by a liquid-crystal template mechanism. *Nature* **1992**, *359*, 710–712.
3. Schuth, F. Engineered porous catalytic materials. *Annu. Rev. Mater. Res.* **2005**, *35*, 209–238.
4. Nooney, R.I.; Kalyanaraman, M.; Kennedy, G.; Maginn, E.J. Heavy metal remediation using functionalized mesoporous silicas with controlled macrostructure. *Langmuir* **2001**, *17*, 528–533.
5. Vallet-Regi, M.; Balas, F.; Arcos, D. Mesoporous materials for drug delivery. *Angew. Chem. Int. Ed.* **2007**, *46*, 7548–7558.
6. Zhao, D.Y.; Feng, J.L.; Huo, Q.S.; Melosh, N.; Fredrickson, G.H.; Chmelka, B.F.; Stucky, G.D. Triblock copolymer syntheses of mesoporous silica with periodic 50 to 300 angstrom pores. *Science* **1998**, *279*, 548–552.
7. Huo, Q.S.; Margolese, D.I.; Ciesla, U.; Feng, P.Y.; Gier, T.E.; Sieger, P.; Leon, R.; Petroff, P.M.; Schuth, F.; Stucky, G.D. Generalized synthesis of periodic surfactant inorganic composite-materials. *Nature* **1994**, *368*, 317–321.
8. Tanev, P.T.; Pinnavaia, T.J. A neutral templating route to mesoporous molecular-sieves. *Science* **1995**, *267*, 865–867.
9. Joo, S.H.; Choi, S.J.; Oh, I.; Kwak, J.; Liu, Z.; Terasaki, O.; Ryoo, R. Ordered nanoporous arrays of carbon supporting high dispersions of platinum nanoparticles. *Nature* **2001**, *412*, 169–172.
10. Yanagisawa, T.; Shimizu, T.; Kuroda, K.; Kato, C. The preparation of alkyltrimethylammonium-kanemite complexes and their conversion to microporous materials. *Bull. Chem. Soc. Jpn.* **1990**, *63*, 988–992.
11. Vartuli, J.C.; Schmitt, K.D.; Kresge, C.T.; Roth, W.J.; Leonowicz, M.E.; McCullen, S.B.; Hellring, S.D.; Beck, J.S.; Schlenker, J.L.; Olson, D.H.; *et al.* Effect of surfactant silica molar ratios on the formation of mesoporous molecular-sieves: Inorganic mimicry of surfactant liquid-crystal phases and mechanistic implications. *Chem. Mater.* **1994**, *6*, 2317–2326.
12. Kresge, C.T.; Roth, W.J. The discovery of mesoporous molecular sieves from the twenty year perspective. *Chem. Soc. Rev.* **2013**, *42*, 3663–3670.
13. Peng, R.; Zhao, D.; Dimitrijevic, N.M.; Rajh, T.; Koodali, R.T. Room temperature synthesis of Ti-MCM-48 and Ti-MCM-41 mesoporous materials and their performance on photocatalytic splitting of water. *J. Phys. Chem. C* **2012**, *116*, 1605–1613.
14. Bronkema, J.L.; Bell, A.T. Mechanistic studies of methanol oxidation to formaldehyde on isolated vanadate sites supported on MCM-48. *J. Phys. Chem. C* **2007**, *111*, 420–430.
15. Boote, B.; Subramanian, H.; Ranjit, K.T. Rapid and facile synthesis of siliceous MCM-48 mesoporous materials. *Chem. Commun.* **2007**, 4543–4545.
16. Huo, Q.S.; Leon, R.; Petroff, P.M.; Stucky, G.D. Mesostructure design with gemini surfactants: Supercage formation in a 3-dimensional hexagonal array. *Science* **1995**, *268*, 1324–1327.

17. Tanev, P.T.; Chibwe, M.; Pinnavaia, T.J. Titanium-containing mesoporous molecular-sieves for catalytic-oxidation of aromatic-compounds. *Nature* **1994**, *368*, 321–323.
18. Wu, P.; Tatsumi, T.; Komatsu, T.; Yashima, T. Postsynthesis, characterization, and catalytic properties in alkene epoxidation of hydrothermally stable mesoporous Ti-SBA-15. *Chem. Mater.* **2002**, *14*, 1657–1664.
19. Anand, R.; Hamdy, M.S.; Gkourgkoulas, P.; Maschmeyer, T.; Jansen, J.C.; Hanefeld, U. Liquid phase oxidation of cyclohexane over transition metal incorporated amorphous 3D-mesoporous silicates M-TUD-1 (M = Ti, Fe, Co and Cr). *Catal. Today* **2006**, *117*, 279–283.
20. Eimer, G.A.; Casuscelli, S.G.; Ghione, G.E.; Crivello, M.E.; Herrero, E.R. Synthesis, characterization and selective oxidation properties of Ti-containing mesoporous catalysts. *Appl. Catal. A* **2006**, *298*, 232–242.
21. Vinu, A.; Srinivasu, P.; Miyahara, M.; Ariga, K. Preparation and catalytic performances of ultralarge-pore Ti-SBA-15 mesoporous molecular sieves with very high Ti content. *J. Phys. Chem. B* **2006**, *110*, 801–806.
22. Blasco, T.; Corma, A.; Navarro, M.T.; Pariente, J.P. Synthesis, characterization, and catalytic activity of Ti-MCM-41 structures. *J. Catal.* **1995**, *156*, 65–74.
23. Koyano, K.A.; Tatsumi, T. Synthesis of titanium-containing mesoporous molecular sieves with a cubic structure. *Chem. Commun.* **1996**, 145–146.
24. Chen, L.Y.; Chuah, G.K.; Jaenicke, S. Ti-containing mcm-41 catalysts for liquid phase oxidation of cyclohexene with aqueous $H_2O_2$ and tert-butyl hydroperoxide. *Catal. Lett.* **1998**, *50*, 107–114.
25. Pena, M.L.; Dellarocca, V.; Rey, F.; Corma, A.; Coluccia, S.; Marchese, L. Elucidating the local environment of Ti(iv) active sites in Ti-MCM-48: A comparison between silylated and calcined catalysts. *Microporous Mesoporous Mater.* **2001**, *44*, 345–356.
26. Ji, D.; Zhao, R.; Lv, G.M.; Qian, G.; Yan, L.; Suo, J.S. Direct synthesis, characterization and catalytic performance of novel Ti-SBA-1 cubic mesoporous molecular sieves. *Appl. Catal. A* **2005**, *281*, 39–45.
27. Berube, F.; Khadhraoui, A.; Janicke, M.T.; Kleitz, F.; Kaliaguine, S. Optimizing silica synthesis for the preparation of mesoporous Ti-SBA-15 epoxidation catalysts. *Ind. Eng. Chem. Res.* **2010**, *49*, 6977–6985.
28. Kumar, A.; Srinivas, D. Selective oxidation of cyclic olefins over framework Ti-substituted, three-dimensional, mesoporous Ti-SBA-12 and Ti-SBA-16 molecular sieves. *Catal. Today* **2012**, *198*, 59–68.
29. Bhaumik, A.; Tatsumi, T. Organically modified titanium-rich Ti-MCM-41, efficient catalysts for epoxidation reactions. *J. Catal.* **2000**, *189*, 31–39.
30. Kholdeeva, O.A.; Derevyankin, A.Y.; Shmakov, A.N.; Trukhan, N.N.; Paukshtis, E.A.; Tuel, A.; Romannikov, V.N. Alkene and thioether oxidations with $H_2O_2$ over Ti-containing mesoporous mesophase catalysts. *J. Mol. Catal. A* **2000**, *158*, 417–421.
31. Zhang, W.Z.; Pinnavaia, T.J. Transition metal substituted derivatives of cubic MCM-48 mesoporous molecular sieves. *Catal. Lett.* **1996**, *38*, 261–265.
32. Ahn, W.S.; Lee, D.H.; Kim, T.J.; Kim, J.H.; Seo, G.; Ryoo, R. Post-synthetic preparations of titanium-containing mesopore molecular sieves. *Appl. Catal. A* **1999**, *181*, 39–49.

33. Kang, K.K.; Ahn, W.S. Physiochemical properties of transition metal-grafted MCM-48 prepared using matallocene precursors. *J. Mol. Catal. A* **2000**, *159*, 403–410.
34. Guidotti, M.; Gavrilova, E.; Galarneau, A.; Coq, B.; Psaroa, R.; Ravasio, N. Epoxidation of methyl oleate with hydrogen peroxide. The use of Ti-containing silica solids as efficient heterogeneous catalysts. *Green Chem.* **2011**, *13*, 1806–1811.
35. Tatsumi, T.; Koyano, K.A.; Igarashi, N. Remarkable activity enhancement by trimethylsilylation in oxidation of alkenes and alkanes with $H_2O_2$ catalyzed by titanium-containing mesoporous molecular sieves. *Chem. Commun.* **1998**, 325–326.
36. Corma, A.; Kan, Q.B.; Rey, F. Synthesis of Si and Ti-Si-MCM-48 mesoporous materials with controlled pore sizes in the absence of polar organic additives and alkali metal ions. *Chem. Commun.* **1998**, 579–580.
37. Corma, A.; Serra, J.M.; Serna, P.; Valero, S.; Argente, E.; Botti, V. Optimisation of olefin epoxidation catalysts with the application of high-throughput and genetic algorithms assisted by artificial neural networks (softcomputing techniques). *J. Catal.* **2005**, *229*, 513–524.
38. Solberg, S.M.; Kumar, D.; Landry, C.C. Synthesis, structure, and reactivity of a new Ti-containing microporous/mesoporous material. *J. Phys. Chem. B* **2005**, *109*, 24331–24337.
39. Guidotti, M.; Pirovano, C.; Ravasio, N.; Lazaro, B.; Fraile, J.M.; Mayoral, J.A.; Coq, B.; Galarneau, A. The use of $H_2O_2$ over titanium-grafted mesoporous silica catalysts: A step further towards sustainable epoxidation. *Green Chem.* **2009**, *11*, 1421–1427.
40. Widenmeyer, M.; Grasser, S.; Kohler, K.; Anwander, R. $TiO_x$ overlayers on MCM-48 silica by consecutive grafting. *Microporous Mesoporous Mater.* **2001**, *44*, 327–336.
41. Zhao, D.; Budhi, S.; Rodriguez, A.; Koodali, R.T. Rapid and facile synthesis of Ti-MCM-48 mesoporous material and the photocatalytic performance for hydrogen evolution. *Int. J. Hydrogen Energy* **2010**, *35*, 5276–5283.
42. Kibombo, H.S.; Zhao, D.; Gonshorowski, A.; Budhi, S.; Koppang, M.D.; Koodali, R.T. Cosolvent-induced gelation and the hydrothermal enhancement of the crystallinity of titania-silica mixed oxides for the photocatalytic remediation of organic pollutants. *J. Phys. Chem. C* **2011**, *115*, 6126–6135.
43. Mahoney, L.; Koodali, R.T. Versatility of evaporation-induced self-assembly (EISA) method for preparation of mesoporous $TiO_2$ for energy and environmental applications. *Materials* **2014**, *7*, 2697–2746.
44. Bandyopadhyay, M.; Birkner, A.; van den Berg, M.W.E.; Klementiev, K.V.; Schmidt, W.; Grunert, W.; Gies, H. Synthesis and characterization of mesoporous MCM-48 containing $TiO_2$ nanoparticles. *Chem. Mater.* **2005**, *17*, 3820–3829.
45. Gao, Y.L.; Konovalova, T.A.; Xu, T.; Kispert, L.A. Electron transfer of carotenoids imbedded in MCM-41 and Ti-MCM-41: EPR, ENDOR, and UV-Vis studies. *J. Phys. Chem. B* **2002**, *106*, 10808–10815.
46. Bal, R.; Chaudhari, K.; Srinivas, D.; Sivasanker, S.; Ratnasamy, P. Redox and catalytic chemistry of Ti in titanosilicate molecular sieves: An EPR investigation. *J. Mol. Catal. A* **2000**, *162*, 199–207.
47. Chaudhari, K.; Srinivas, D.; Ratnasamy, P. Reactive oxygen species in titanosilicates TS-1 and TiMCM-41: An *in situ* EPR spectroscopic study. *J. Catal.* **2001**, *203*, 25–32.

48. Chaudhari, K.; Bal, R.; Srinivas, D.; Chandwadkar, A.J.; Sivasanker, S. Redox behavior and selective oxidation properties of mesoporous titano- and zirconosilicate MCM-41 molecular sieves. *Microporous Mesoporous Mater.* **2001**, *50*, 209–218.
49. Wu, C.M.; Peng, R.; Dimitrijevic, N.M.; Rajh, T.; Koodali, R.T. Preparation of $TiO_2$-$SiO_2$ aperiodic mesoporous materials with controllable formation of tetrahedrally coordinated $Ti^{4+}$ ions and their performance for photocatalytic hydrogen production. *Int. J. Hydrogen Energy* **2014**, *39*, 127–136.
50. Liu, Z.F.; Crumbaugh, G.M.; Davis, R.J. Effect of structure and composition on epoxidation of hexene catalyzed by microporous and mesoporous Ti-Si mixed oxides. *J. Catal.* **1996**, *159*, 83–89.
51. Tuel, A.; Hubert-Pfalzgraf, L.G. Nanometric monodispersed titanium oxide particles on mesoporous silica: Synthesis, characterization, and catalytic activity in oxidation reactions in the liquid phase. *J. Catal.* **2003**, *217*, 343–353.
52. Hutter, R.; Mallat, T.; Baiker, A. Titania-silica mixed oxides: II. Catalytic behavior in olefin epoxidation. *J. Catal.* **1995**, *153*, 177–189.
53. Dellarocca, V.; Marchese, L.; Pena, M.L.; Rey, F.; Corma, A.; Coluccia, S. Surface Properties of Mesoporous Ti-MCM-48 and Their Modifications Produced by Silylation. In Proceedings of Oxide-based Systems at the Crossroads of Chemistry—Second International Workshop, Como, Italy, 8–11 October, 2000, Gamba, A., Colella, C., Coluccia, S., Eds.; Elsevier Science B.V.: Amsterdam, The Netherlands, 2001; pp. 209–220.